The Journal of Neuroscience, August 15, 2000, *20*(16):5899–5905

Developmental Profile of the Changing Properties of NMDA Receptors at Cerebellar Mossy Fiber–Granule Cell Synapses

Laurence Cathala, Charu Misra, and Stuart Cull-Candy

Department of Pharmacology, University College London, London WC1E 6BT, United Kingdom

During cerebellar development, granule cells display well characterized changes in the expression of NMDA receptor (NMDAR) NR2 subunits, switching from NR2B to NR2A and NR2C in mature cells. Although various studies, including experiments on mutant mice with one or more NR2 subunit types deleted, suggest that NR2A, NR2B, and NR2C subunits contribute to synaptic NMDARs, changes in the properties of the mossy fiber EPSC during development have not been fully evaluated. In particular, information on NMDAR EPSCs in mature animals is lacking. We have examined pharmacological and kinetic properties of NMDARs at mossy fiber–granule cell synapses from their formation to maturity [postnatal day 7 (P7)–P40 rats]. Significant changes were seen in the relative amplitudes of the non-NMDAR- and NMDAR-mediated components of the evoked EPSC and in the decay kinetics of the latter. The NMDA/non-NMDA ratio was similar at P7, P21, and P40, but showed a clear peak at P12. This change coincided with a speeding of the NMDAR EPSC decay, accompanied by a decrease in sensitivity to ifenprodil (selective NR2B-antagonist). By P21, sensitivity of the NMDAR EPSC to Mg^{2+} was approximately threefold less than that at P12 (IC_{50}, 76 vs 28 μM), suggesting incorporation of the NR2C subunit. However, the predicted slowing of decay kinetics to a value more characteristic of NR2C deactivation, was not seen until P40. Our data are consistent with the known switch from NR2B to NR2A subunits during the first two postnatal weeks, but suggest a gradual incorporation of the NR2C subunit that modifies Mg^{2+} sensitivity and only later influences EPSC kinetics.

Key words: cerebellum; granule cells; NMDA receptors; synaptic transmission; patch-clamp; NMDA subunit expression; NR2C subunit

The neurotransmitter L-glutamate activates NMDA receptors (NMDARs) at many synapses in the vertebrate CNS. These receptors are modulated by various endogenous molecules, including Mg^{2+}, glycine, Zn^{2+}, and protons. Furthermore, they display high Ca^{2+} permeability and slow deactivation kinetics (Dingledine et al., 1999). These characteristic attributes are governed by the types of NR1 and NR2 subunits forming the receptor (Monyer et al., 1994; Feldmeyer and Cull-Candy, 1996). The time course and pharmacology of the NMDAR-mediated component of EPSCs (NMDAR EPSCs) can display striking changes during development (Carmignoto and Vicini, 1992; Hestrin, 1992), primarily as a result of changes in the type of NR2 subunit present. For example, a switch from NR2B- to NR2A-containing receptors has been described, resulting in acceleration of NMDAR EPSCs (Takahashi et al., 1996; Rumbaugh and Vicini, 1999; Tovar and Westbrook, 1999) and a reduction in synaptic plasticity (Carmignoto and Vicini, 1992; Quinlan et al., 1999) at a number of central synapses.

In the present study we aimed to determine the effect of subunit changes on the properties of synaptic NMDARs at the cerebellar mossy fiber–granule cell synapse. The early expression of NR2B in granule cells is replaced by NR2A and later by intense expression of mRNA for NR2C. The finding that the level of NR2C mRNA is unusually high in granule cells from adult animals, in contrast with its sparse expression elsewhere in the CNS (Akazawa et al., 1994; Monyer et al., 1994), has provided a further stimulus to understanding its properties at the mossy fiber synapse. Studies of recombinant receptors indicate that the NR2C subunit forms NMDARs with a low sensitivity to Mg^{2+} block, compared with NMDARs that contain NR2A or NR2B subunits (Kuner and Schoepfer, 1996). NR2C-containing NMDARs (low-conductance NMDAR channels) can be readily detected in somatic patches from granule cells in animals aged postnatal day 19 (P19) or older, typically occurring along with the high-conductance NR2A- or NR2B-containing NMDARs (Farrant et al., 1994). Although studies on 1- to 3-week-old animals, including experiments on mutant mice with one or more NR2 subunit types deleted, suggest that NR2A, NR2B, and NR2C subunits can all contribute to synaptic NMDARs (Ebralidze et al., 1996; Kadotani et al., 1996; Takahashi et al., 1996), changes in the properties of the mossy fiber EPSC over a wide developmental period have not been fully evaluated. Furthermore, there is little information on granule cell NMDAR EPSCs in mature animals.

We therefore, examined the properties of evoked EPSCs at the mossy fiber-to-granule cell synapse from the time of its formation to maturity. We show that NMDAR EPSCs are present throughout this developmental period and that mature granule cell synapses display features that differ from other synapses in the CNS. During the initial 3 weeks of postnatal development, the decay of NMDAR EPSCs was markedly accelerated, consistent with insertion of NR2A- and gradual loss of NR2B-containing receptors. Our experiments indicate that from the third postnatal week NR2C-containing NMDARs make a major functional contribution to the mossy fiber–granule cell synapse, conferring a reduced sensitivity to Mg^{2+}, followed by a prolongation in time course of the NMDAR EPSC in the mature animal.

MATERIALS AND METHODS

Slice preparation. Parasaggital slices (200–300 μm) were cut from the cerebellum of Sprague Dawley rats between P7 and P40 as described previously (Farrant et al., 1994). Briefly, rats were decapitated, and the brain was rapidly removed and placed in cold "slicing" (2–4°C) solution of the following composition (mM): NaCl 125; KCl 2.5; $CaCl_2$ 1; $MgCl_2$ 2; $NaHCO_3$ 26; NaH_2PO_4 1.25; glucose 25, pH 7.4, when bubbled with 95% O_2 and 5% CO_2. Slices were cut from the dissected cerebellar vermis using a moving blade microtome (DTK-1000; Dosaka EM Company, Kyoto, Japan); these were incubated in slicing solution at 30°C for 1 hr and subsequently were maintained at room temperature for up to 8 hr. For electrophysiological experiments, the slices were transferred to a chamber on a fixed-stage Axioskop microscope (Zeiss, Welwyn Garden City, UK) and examined at room temperature (22–25°C). Granule cells were viewed

Received March 8, 2000; revised May 10, 2000; accepted May 19, 2000.

This work was supported by the Wellcome Trust. L.C. gratefully acknowledges receipt of a Wellcome Travelling Fellowship, and C.M. gratefully acknowledges receipt of a Wellcome Prize Fellowship. We thank Stephen Brickley, Beverley Clark, and Mark Farrant for valuable discussions and comments on this manuscript.

Correspondence should be addressed to Stuart Cull-Candy, University College London, Gower Street, London WC1E 6BT, UK. E-mail: s.cull-candy@ucl.ac.uk.

 0270-6474/00/205899-07$15.00/0

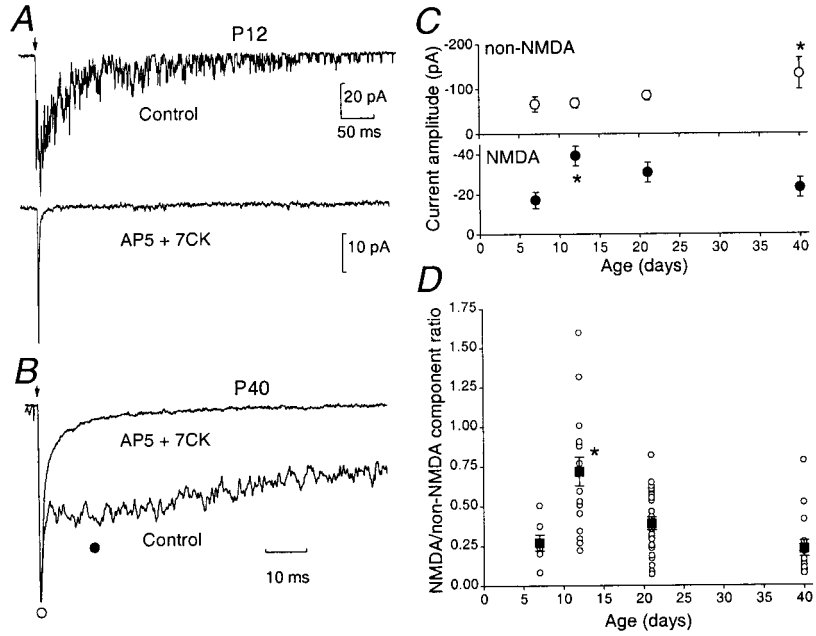

Figure 1. Age-dependent changes in the amplitude of non-NMDAR and NMDAR EPSCs. *A*, A single control EPSC recorded at P12 (−80 mV) showing an initial non-NMDAR component followed by a NMDAR component (*top panel*). The NMDAR EPSC was abolished in the presence of 50 μM AP-5 and 50 μM 7-CK (*bottom panel*), leaving the non-NMDAR-component. *B*, Average traces of consecutive EPSCs at P40 displayed on a faster time scale, indicating a clear separation of the NMDAR and non-NMDAR components. The amplitude of the non-NMDAR EPSC was measured at its peak (*open circle*); the NMDAR EPSC was measured 10 msec after the peak from a 1 msec epoch (*filled circle*). Traces are averaged from at least 20 evoked EPSCs and normalized to the peak. *C*, Amplitudes of the non-NMDAR (*top panel*) and NMDAR component (*bottom panel*) for each age group (n = 7 at P7, n = 17 at P12, n = 28 at P21, and n = 16 at P40). *D*, Amplitude ratio of NMDAR versus non-NMDAR component of the different age groups. For each age group, the ratio is indicated for each recorded cell (*open circle*); the average from each age group is indicated by a *closed square* (error bars indicate SEM). Note that at P12, the NMDAR EPSC is prominent, sometimes exceeding that of the non-NMDAR component.

under Nomarski differential interference optics (40× water-immersion objective; total magnification, 320–1000×), and identified from their appearance and their characteristic electrical properties.

Solutions and drugs. Slices were perfused with external solution, which differed from slicing solution in lacking Mg^{2+}. The internal (pipette) solution used for recording contained (mM): CsF, 110; CsCl, 30; HEPES, 10; EGTA, 5; NaCl, 4; $CaCl_2$, 0.5; and Mg-ATP, 2, adjusted to pH 7.3 with CsOH.

Mossy fiber-evoked EPSCs were examined in isolation by blocking both GABAergic and glycinergic receptors with 100 μM picrotoxin. A 10 μM concentration of glycine was added to the bathing solution to facilitate NMDAR activation. In outside-out patch recordings, the following drugs were added to the Mg^{2+}-free external solution: 1 μM strychnine and 10 μM bicuculline to block glycinergic and GABAergic receptors, respectively. Additionally, 5 μM 6-cyano-7-dinitroquinoxalinedione (CNQX) and 300 nM tetrodotoxin (TTX) were added to block AMPA receptors and voltage-activated sodium channels. For activation of NMDARs in patches, 10 μM NMDA was applied together with 10 μM glycine.

All salts were obtained from Sigma (Poole, UK), and BDH Chemicals (Poole, UK). The following drugs were used: bicuculline methobromide (Research Biochemicals, Natick, MA), CNQX, D-2-amino-5-phosphonopentanoic acid (AP-5), 7-chloro-kynurenate (7-CK), NMDA (Tocris Cookson, Bristol, UK), glycine (BDH Chemicals), *N-N-N′-N′*-tetrakis-(2-pyridylmethyl)-ethylenediamine (TPEN), TTX, 6,7-dinitroquinoxaline-2,3-dione (DNQX), ifenprodil, picrotoxin, and strychnine hydrochloride (Sigma).

Recording procedures. All patch-clamp recordings were made using an Axopatch-200A or 200B amplifier (Axon Instruments, Foster City, CA). Patch pipettes were made from thick-walled borosilicate glass tubing (GC-150F; Clark Electromedical, Pangbourne, UK). Pipettes were coated with Sylgard resin (Dow Corning 184) and fire-polished to a resistance of 8–10 MΩ for whole-cell recordings or 10–12 MΩ for single-channel recordings. Series resistance and capacitance measures were determined directly from the amplifier settings. Series resistance compensation was not used. Cell capacitance was: 4.7 ± 0.4 pF (n = 10) at P7, 3.5 ± 0.09 pF (n = 28) at P12, 3.2 ± 0.16 pF (n = 40) at P21, and 3.4 ± 0.2 pF (n = 14) at P40. Series resistance was: 16.5 ± 0.8 MΩ at P7, 18 ± 1 MΩ at P12, 20 ± 0.8 MΩ at P21, and 20 ± 1.5 MΩ at P40. Solutions were bath-applied via gravity feed. Afferent inputs (mossy fibers) were stimulated via a glass pipette (~30 μm diameter) filled with external solution. This was positioned in the white matter and a pulse of at least 10 μsec duration was delivered at 0.1 Hz (Neurolog DS2; Digitimer Limited). The intensity of the stimulation was set at just suprathreshold.

Data analysis. Current records were stored on digital audiotape (DTR-1204; BioLogic, Claix, France; DC to 20 kHz). EPSCs were filtered at 2 kHz (−3 dB, eight pole lowpass Bessel filter), and digitized at 20 kHz (digidata 1200; pClamp versions 6 and 8; Axon Instruments). Single-channel currents were filtered at 2 kHz and digitized at 10 kHz.

Evoked EPSCs were analyzed using Axograph (Axon Instruments). Average waveforms (from at least 20 sweeps) were constructed by aligning EPSCs on the stimulus artifact. We used two methods to analyze the NMDAR component: (1) The amplitude of the NMDAR EPSC was measured 10 msec after the non-NMDAR peak (average of 28 points), and (2) the charge transfer, after subtraction of the non-NMDAR-component (charge remaining in the presence of 50 μM AP-5 and 50 μM 7-CK), was measured by integrating the EPSC. The decays of the non-NMDAR or NMDAR-mediated component of evoked EPSCs were fitted separately and each were best described by the sum of two exponential functions: $A(t) = A_{slow} \exp(-t/\tau_{slow}) + A_{fast} \exp(-t/\tau_{fast})$, where τ_{slow} and τ_{fast} are the decay time constants of the slow and fast component and A_{slow} and A_{fast} are their respective amplitudes.

To fit the NMDAR EPSC decay, the amplitude was normalized to a value measured 10 msec after the peak of the non-NMDAR component, and the remaining portion of the current was fitted (see Fig. 2*A*). To compare the decay of EPSCs at different ages, the weighted time constant (τ_w) was used: $\tau_w = \tau_{slow}[A_{slow}/(A_{slow} + A_{fast})] + \tau_{fast}[A_{fast}/(A_{slow} + A_{fast})]$.

For analysis of single-channel records, consecutive 100 msec epochs of NMDAR channel activity were integrated, and the average charge transfer in the presence and absence of drug was calculated using the program N05 (Stephen Traynelis, Emory University, Atlanta, GA). The effect of ifenprodil was calculated by comparing the average charge transfer during control periods and in the presence of ifenprodil. Graphs were constructed in Origin (version 4.1, Microcal, Northampton, MA).

Mg^{2+} inhibition curves were fitted with a form of the Hill equation: $I = I_{max}/(1 + ([A]/IC_{50})^n + (100 - I_{max})$, where I_{max} is the maximal inhibition of the response, $[A]$ is the concentration of Mg^{2+}, IC_{50} is the concentration of Mg^{2+} required to reduce the response to 50% of control, and n is the Hill slope (set to 1).

Average data are expressed as mean ± SEM (n = number of cells or patches). Statistical significance between groups was tested using the two-tailed Student's t test and were considered significant at $p < 0.05$.

RESULTS

Age-dependent changes in EPSC amplitude in granule cells

EPSCs were examined at the mossy fiber–granule cell synapse in cerebellar slices from rats aged between P7 and P40 (n = 68 cells). By P40, mossy fiber synapses have reached the adult level of organization (Hamori and Somogyi, 1983), and granule cells have attained their adult pattern of NMDAR subunit mRNA expression (Akazawa et al., 1994; Monyer et al., 1994; Watanabe et al., 1994).

Figure 1 shows typical two-component EPSCs evoked by mossy fiber stimulation at P12 (single EPSCs; Fig. 1*A*) and P40 (Fig. 1*B*; average EPSCs; V_H = −80 mV). The initial fast non-NMDAR component could be readily blocked by CNQX (5 μM; n = 3) or DNQX (10 μM; n = 6; data not shown), leaving a slow NMDAR component. As shown in Figure 1, *A* and *B*, this could be abolished in both young and mature animals by the NMDAR antagonists AP-5 (50 μM) and 7-CK (50 μM; n = 37) (Silver et al., 1992; Takahashi et al., 1996; Clark et al., 1997). The non-NMDAR EPSCs showed a gradual age-dependent increase in amplitude. This component was significantly larger at P40 (Fig. 1*C, top panel*) but showed little change in its decay kinetics (weighted decay time constant τ_w = 2.3 ± 0.4 msec at P7, 2.1 ± 0.2 at P12, 2.4 ± 0.4 msec at P21, and 2.2 ± 0.4 msec at P40). To analyze the amplitude of NMDAR EPSCs, we measured this event 10 msec after the EPSC

peak (Fig. 1*B*). As is apparent in Figure 1*C* (*bottom panel*), the NMDAR EPSCs were similar in amplitude at P7 and P40, with a transient, but significant, increase at P12.

The ratio of NMDAR- versus non-NMDAR EPSC amplitudes was similar at P7, P21, and P40 (Fig. 1*D*). However, this was significantly greater at P12 ($p < 0.05$). Previous work has demonstrated that the NMDAR- versus non-NMDAR EPSC ratio decreases between P10 and P22 (D'Angelo et al., 1993). However, our examination of a wide range of ages has indicated that this apparent decrease in the ratio reflects a transient increase in the NMDAR-mediated component at P12 and that this component (and hence the NMDAR- vs non-NMDAR EPSC ratio) was not significantly changed at the mature synapse. The cause of the change at P12 is uncertain, although it could reflect an increase in the open probability or density of the postsynaptic NMDARs. Furthermore, it may be a consequence of the change in glomerular structure during this critical period of synapse formation (P12–P15). Indeed, during this time both the synaptic junction perimeter and the number of active sites increase (Hamori and Somogyi, 1983), the latter being associated with an increase in spillover of transmitter between release sites (Silver et al., 1996). This could contribute to the transient increase in NMDAR EPSC amplitude at P12.

Developmental changes in the decay kinetics of NMDAR EPSCs

We next examined the developmental change in NMDAR EPSC decay kinetics. Figure 2*A* shows examples of averaged EPSCs recorded at P7, P21, and P40. The NMDAR EPSC decay times were noticeably faster at P21 than at either P7 or P40. At all ages, the decay phase of the NMDAR EPSC could be well fitted by the sum of two exponentials (τ_{slow} and τ_{fast}; Table 1). The change in the weighted mean decay time (τ_w) of the NMDAR EPSC is illustrated in Figure 2*B*. The decay was slow at P7 ($\tau_w = 147 \pm 10$ msec; $n = 7$), but accelerated significantly to 77 ± 6 msec at P12 ($n = 15$) and 75 ± 7 msec at P21 ($n = 11$). However, by P40 τ_w was prolonged to 147 ± 13 msec ($n = 10$)—comparable to that observed at P7. These changes in τ_w were mainly because of a change in τ_{slow}. Thus, although τ_{fast} accounted for ~70% of the current, its time course and amplitude were not significantly different at the various ages examined (Table 1, Fig. 2*C*). However, τ_{slow} exhibited an approximately twofold decrease between P7 and 12, whereas its value at P40 was similar to that at P7. There was no significant difference between the τ_{slow} values observed at P7 and P40 or between values at P12 and P21 (Table 1, Fig. 2*C*).

In situ hybridization studies have indicated that NR2B mRNA is present in granule cells only in the first and second postnatal weeks (Akazawa et al., 1994; Monyer et al., 1994; Watanabe et al., 1994). Furthermore the NR2B protein in cerebellar tissue is reduced with age (Takahashi et al., 1996; Wenzel et al., 1997), being replaced by NR2A and NR2C subunits (Wenzel et al., 1997). To determine whether the change in NMDAR EPSC decay kinetics could be directly ascribed to changes in the subunit composition of synaptic NMDARs, we examined the effect of subunit-selective drugs and Mg^{2+} ions on NMDAR EPSCs.

Effect of NR1/NR2B selective blocker ifenprodil on EPSCs

Ifenprodil acts as an atypical noncompetitive NMDAR antagonist that selectively interacts with NR2B-containing NMDARs (Williams, 1993, 1995; Gallagher et al., 1996) and has been extensively used to assess the presence of the NR2B subunit at central synapses (Cull-Candy et al., 1998; Stocca and Vicini, 1998; Quinlan et al., 1999; Tovar and Westbrook, 1999; Misra et al., 2000a).

Figure 3 compares EPSCs in the presence and absence of ifenprodil (10 μM) at P7, P12, and P21. Whereas ifenprodil reduced the amplitude of the NMDAR EPSC at all ages, the strong inhibition apparent at P7 decreased progressively with age. The percentage inhibition was significantly less at P21 versus P7 ($p < 0.05$; Fig. 3*D*). Indeed, in some cells ifenprodil produced a barely detectable reduction by P21 (Fig. 3*C*). These observations suggest that in young animals NMDAR EPSCs are mediated largely by NR2B-containing NMDARs, but by P21 these make a relatively small contribution. This is in keeping with our previous experiments on P21 knock-out mice lacking the NR2A subunit, in which the NR2B protein had declined to ~20% of its maximum level and the high-conductance (NR2B-containing) channels represented only ~15% of openings at this age (Takahashi et al., 1996). Similarly, recent experiments by Rumbaugh and Vicini (1999) have shown that NMDAR EPSCs are inhibited in an age-dependent manner by the NR2B-selective antagonist CP 101,606.

Expression of mRNA for the NR2A subunit begins during the second postnatal week (Akazawa et al., 1994; Monyer et al., 1994). Because recombinant NR1/NR2A receptors are insensitive to ifenprodil, it seemed likely that NMDAR EPSCs observed in the presence of ifenprodil in older animals reflected an increased expression of NR2A-containing NMDARs. To confirm this, we examined the effect of the Zn^{2+} chelator TPEN on whole-cell NMDA responses. TPEN has previously been shown to potentiate, by up to threefold, the response of recombinant NR2A-containing

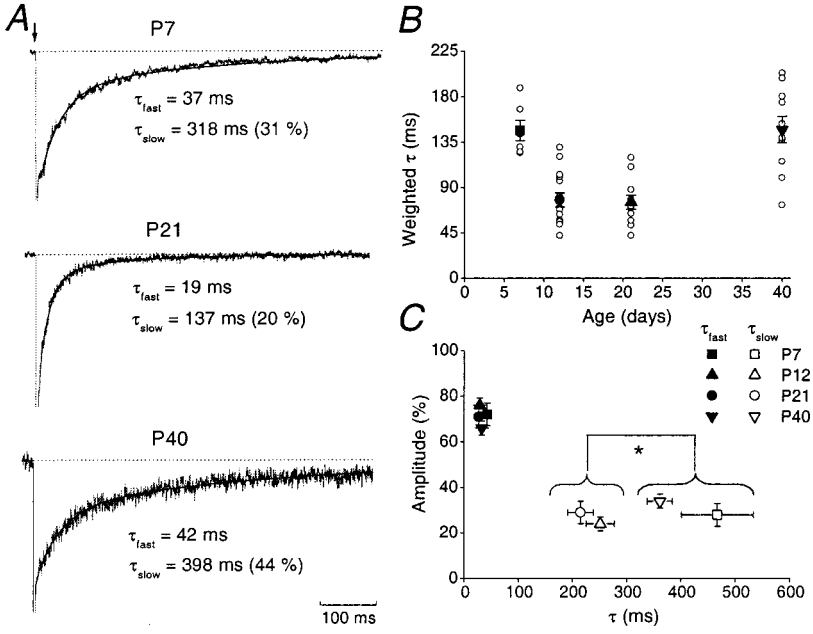

Figure 2. Age-dependent changes in decay kinetics of NMDAR EPSCs. *A*, Representative normalized averaged NMDAR EPSCs at P7, P21, and P40. In all cases, the decay was best fitted by a double exponential function. The fitted functions are superimposed (*black line*) with their τ_{fast} and τ_{slow} values indicated. *B*, Plot of weighted τ (τ_ω) versus age. Note that values of τ_ω at P7 and P40 are significantly different from those at P12 and P21. For each age group, individual cells are indicated by an *open circle*, and the average from each age group is indicated by a *closed symbol* (error bars indicate SEM). *C*, Relative amplitude (in percentage) of fast and slow components versus time constant of decay. For each age group the mean τ_{fast} and the mean τ_{slow} are plotted versus their relative contribution to the total NMDAR EPSC.

Table 1. Decay time constants of the NMDAR-EPSCs at different stages of development (P7–P40)

	τ_{fast} (msec)	A_{fast} (%)	τ_{slow} (msec)	A_{slow} (%)
P7 ($n = 6$)	42 ± 3	72 ± 5	467 ± 66	28 ± 5
P12 ($n = 15$)	29 ± 2	76 ± 3	251 ± 26	24 ± 3
P21 ($n = 11$)	27 ± 3	71 ± 5	215 ± 24	29 ± 5
P40 ($n = 10$)	32 ± 3	66 ± 3	361 ± 22	34 ± 3

The fast (τ_{fast}) and slow (τ_{slow}) decay time constant values obtained from the double exponential fit are presented, together with the relative contribution of each component to total NMDAR EPSC. The amplitude of fast (A_{fast}) and slow components (A_{slow}) are expressed as a percentage of total NMDAR EPSC.

NMDARs, whereas having little effect on other NR2-containing NMDARs (Paoletti et al., 1997). TPEN (1 μM) potentiated NMDA (10 μM)-evoked currents at P6 by 38 ± 1% ($n = 15$; $p < 0.05$), suggesting an early contribution of the NR2A subunit to granule cell NMDARs (data not shown).

These pharmacological properties, together with the NMDAR EPSC decay kinetics, support the idea that both NR2B and NR2A subunits are present at immature mossy fiber synapses. This conclusion is also consistent with our earlier observation that high-conductance (50 pS) NMDAR channels underlie the NMDAR EPSC at ~P12 (Clark et al., 1997). Our τ_{slow} value for NMDAR EPSCs at P7 approximates to the deactivation time of ~400 msec reported for recombinant NR2B-containing NMDARs, consistent with the strong ifenprodil block at this stage. Our τ_{slow} values at P12–P21 were close to the fast deactivation value (τ ~120 msec) reported for recombinant NR2A-containing NMDARs (Monyer et al., 1994; Vicini et al., 1998). Moreover, the relative amplitude we obtained for the fast-decaying component of the NMDAR EPSC (~70–75%) is within the range described for recombinant NR1/NR2A receptors (~60–90%; Vicini et al., 1998; Wyllie et al., 1998) and approaches the value of ~80% reported by Ebralidze et al., (1996) at this synapse in P14–P18 mice lacking the NR2C subunit. However, it seems unlikely that the NMDAR EPSC in P12–P21 rats arose from pure NR1/NR2A receptors, given the fact that they were still markedly reduced by ifenprodil at P12 and exhibited a low sensitivity to Mg^{2+} at P21 (see below). It is also of note that our value for τ_{slow} at P40 matches the deactivation kinetics (τ, ~380 msec) reported for recombinant NR2C-containing NMDARs (Monyer et al., 1994).

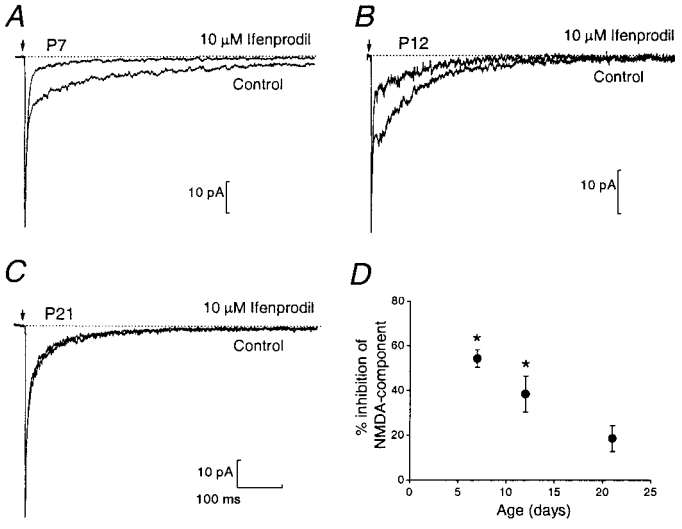

Figure 3. Ifenprodil block of the NMDAR EPSC decreases with age. *A–C*, Average evoked EPSCs before and during bath application of 10 μM ifenprodil at P7 (*A*), P12 (*B*), and P21 (*C*). Note that only the NMDAR EPSC was reduced by ifenprodil. *D*, Mean percentage inhibition of the NMDAR EPSC induced by ifenprodil in the different age groups. The percentage inhibition was estimated by comparing the amplitude of the NMDAR EPSC 10 msec after the non-NMDAR peak in control conditions and 2 min after the onset of drug application. The percentage inhibition decreased significantly with age from 55 ± 4% at P7 ($n = 6$; $p < 0.05$) to 38 ± 8% at P12 ($n = 6$; $p < 0.05$) and 18 ± 6% at P21 ($n = 6$; $p > 0.05$).

Ifenprodil block of extrasynaptic NMDARs decreased with age

For comparison with synaptic data, we also examined the effect of ifenprodil on somatic patches at P7, P12, and P21. Bath application of 10 μM NMDA (with 10 μM glycine) resulted in clear single-channel activity in all outside-out patches analyzed (Farrant et al., 1994). As illustrated in Figure 4*A*, the single-channel activity at P7 was significantly reduced (although not completely blocked) by 10 μM ifenprodil. Residual channel openings were clearly briefer in duration (Fig. 4*B*), as previously described for recombinant NR1/NR2B receptors (Williams, 1993; Priestley et al., 1995) and for native NMDARs (Legendre and Westbrook, 1991). By P21, the effect of ifenprodil on patches was markedly reduced (Fig. 4*B*). We examined the effect in more detail by comparing mean charge transfer through single NMDAR channels, in control conditions and in 10 μM ifenprodil. Figure 4*C* shows examples of measurements obtained by integrating consecutive 100 msec epochs of channel activity at P7 and P21. The effect of ifenprodil on charge transfer was significantly reduced by P21. As shown in Figure 4*D*, there was a significant difference in the percentage of inhibition at P7 versus P21 ($p < 0.05$).

The presence of residual NMDAR-channel activity at P7 in ifenprodil-treated patches does not necessarily imply that the remaining events arose from other NMDAR subtypes, because ifenprodil produces only ~80% block in a pure population of recombinant NR1/NR2B receptors (Williams, 1993; Priestley et al., 1995; Tovar and Westbrook, 1999). The gradual age-dependent reduction in ifenprodil sensitivity of extrasynaptic NMDAR channels was comparable to that of synaptic NMDARs activated during the EPSC (compare Figs. 3*D* and 4*D*; but see Rumbaugh and Vicini, 1999).

Age-dependent shift in IC_{50} for Mg^{2+} block of synaptic NMDARs

Voltage-dependent block of the NMDAR pore by extracellular Mg^{2+} ions (Mayer et al., 1984; Nowak et al., 1984) is critical in allowing synaptic NMDARs to act as coincidence detectors (for review, see Malenka and Nicoll, 1999). The degree of block produced by Mg^{2+} is much less for NR2C- than for NR2A- or NR2B-containing recombinant receptors (Monyer et al., 1994; Kuner and Schoepfer, 1996). From the second postnatal week granule cells express mRNA for the NR2C subunit, and we have previously shown that NR2C-containing NMDARs can be detected in the soma of these cells (Farrant et al., 1994). Earlier studies on mutant mice, by ourselves and others (Ebralidze et al., 1996; Takahashi et al., 1996), have indicated that both NR2A and NR2C subunits may contribute to EPSCs by the end of the third postnatal week. In the present study, the slowing of the NMDAR EPSC at P40 suggests a relatively late appearance of NR2C-containing receptors at the synapse. To examine this question further we tested the effect of Mg^{2+} on NMDAR EPSCs at P12, P21, and P40.

Figure 5*A* shows evoked EPSCs at P12 and P21, normalized to the peak of the non-NMDAR component and superimposed to allow comparison of the NMDAR components. Mg^{2+} produced a concentration-dependent block of the NMDAR EPSC. The degree of block produced by 0.03 and 0.1 mM Mg^{2+} was greater at P12 than at P21. We estimated the mean charge transfer carried by synaptic NMDARs by integrating NMDAR EPSCs (see Materials and Methods). Charge transfer was determined over a range of Mg^{2+} concentrations (0.01–2 mM); the inhibition curves obtained from this analysis are depicted in Figure 5*B*. These were fitted by the Hill equation and had a single component. At P21, there was an approximately threefold shift in the IC_{50} toward higher Mg^{2+} concentrations. The mean IC_{50} values were 28 ± 2 μM at P12, and 76 ± 8 μM at P21: these were significantly different ($p < 0.05$).

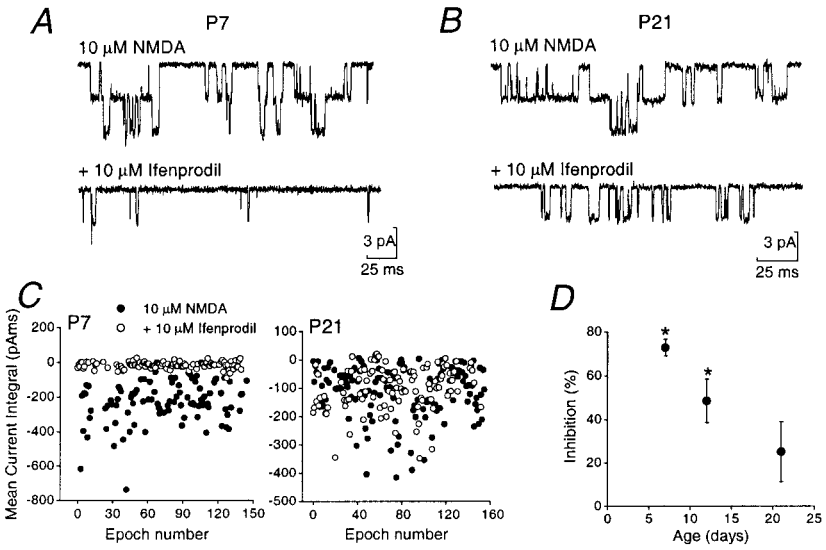

Figure 4. Effect of ifenprodil on single-channel currents in outside-out patches from granule cells of different ages. *A*, *B*, Recordings at P7 and P21 in response to 10 μM NMDA (and 10 μM glycine). The *bottom trace* of each pair illustrates channel openings from the same cell in the presence of 10 μM ifenprodil. *C*, Plots of mean current integral of single-channel activity, in the absence and presence of ifenprodil. Each *dot* represents charge transfer during a 100 msec epoch (*filled circles*). At P7, ifenprodil markedly reduced charge transfer (*open circles*). At P21 charge transfer was largely unaffected by ifenprodil. *D*, Plot summarizing percentage inhibition of channel activity by ifenprodil in patches from granule cells of various ages. The percentage of inhibition decreased significantly with age, from 73 ± 4% at P7 ($n = 6$; $p < 0.05$), to 48 ± 10% at P12 ($n = 7$; $p < 0.05$), and 25 ± 14% at P21 ($n = 6$; $p > 0.05$).

We also examined granule cells at P40. Because of the difficulty in recording from P40 cells for the time required to construct a full inhibition curve we examined the effect of a single Mg^{2+} concentration, chosen to fall approximately on the midpoint of the curve. A concentration of 0.1 mM Mg^{2+} produced 37 ± 7% inhibition of NMDAR EPSCs ($n = 4$; Fig. 5*B*). This degree of inhibition was not significantly different from that observed at P21 for the same Mg^{2+} concentration, indicating that the Mg^{2+} sensitivity of NMDAR EPSCs exhibited little further change with age. The reduced Mg^{2+} sensitivity, observed from P21 onward, together with the increased duration of the NMDAR EPSC at P40, suggests that NR2C subunits make a major contribution to the properties of the NMDAR EPSCs at the mature mossy fiber–granule cell synapse.

DISCUSSION

Our experiments have identified distinct changes in the functional and pharmacological properties of NMDAR EPSCs at the mossy fiber–granule cell synapse. These observations have several broad implications for the role of NMDARs in granule cells, particularly with respect to the influence of the NR2C subunit at the mature synapse. First, we find functional evidence for the early loss of NR2B and insertion of NR2A subunits. Second, our observations demonstrate a pronounced slowing in time course of the NMDAR EPSC in the mature cells consistent with incorporation of the NR2C subunit. Third, our results suggest that the influence of the NR2C subunit on the Mg^{2+} sensitivity of synaptic NMDARs precedes its effects on NMDAR decay kinetics. These various aspects are considered below.

Our experiments indicate that during the first postnatal week the properties of NMDAR EPSCs in granule cells are governed by the NR2B subunit. By the second postnatal week, the speeding up of the NMDAR EPSC, together with the increased TPEN sensitivity and decreased ifenprodil sensitivity, suggests an increasing contribution from the NR2A subunit. These changes in kinetic and pharmacological properties correlate well with the known changes in mRNA expression pattern within the cerebellum (Akazawa et al., 1994; Monyer et al., 1994; Watanabe et al., 1994). Furthermore, they resemble the developmental switch from NR2B to NR2A that occurs at a number of central synapses in early CNS development, resulting in shortening of the NMDAR EPSC (Quinlan et al., 1999; Roberts and Ramoa, 1999; Rumbaugh and Vicini, 1999; Tovar and Westbrook, 1999).

Our data indicate that the NR2A subunit, along with the NR2B subunit, contribute to synaptic NMDARs soon after synapse formation (from P7). Indeed, we found that, whereas ifenprodil markedly reduced NMDAR EPSC amplitude at the end of the first postnatal week, the magnitude of block was less than expected if NR2B was the only NR2 subunit present (Tovar and Westbrook, 1999). The progressive reduction in ifenprodil sensitivity, to low levels by the end of the third postnatal week, indicate a gradual switch from NR2B to NR2A at the immature granule cell synapse. It is not clear whether this pharmacological change and acceleration of the NMDAR EPSC reflects an increase in the relative proportion of NR1/NR2A receptors (with concomitant decrease in NR1/NR2B receptors), or the formation of triheteromeric NR1/NR2A/NR2B receptors (Vicini et al., 1998), or a mixture of both diheteromeric and triheteromeric assemblies. Interestingly, the presence of highly ifenprodil-sensitive (NR1/NR2B receptors) extrasynaptic NMDARs together with a population of less ifenprodil-sensitive synaptic receptors in hippocampal cells, had led to the suggestion that diheteromeric and triheteromeric (NR1/NR2A/NR2B) can coexist within cells (Tovar and Westbrook, 1999). The age-dependent reduction in ifenprodil sensitivity that we observed for extrasynaptic receptors was comparable to that seen at the synapse. This contrasts with the results of Rumbaugh and Vicini (1999), obtained using another NR2B-selective antagonist (CP 101,606), who have suggested that the loss of NR2B-containing NMDARs occurs more rapidly at the synapse. The reason for this difference is not clear.

Cerebellar granule cells express high levels of mRNA for the NR2C subunit in rats older than ~P11 (Akazawa et al., 1994; Watanabe et al., 1994). Furthermore, somatic patches from >P19 granule cells give rise to channel openings with the characteristically low single-channel conductance typical of NR2C-containing receptors (~18 and 35 pS; Farrant et al., 1994). Experiments on knock-out mice (Ebralidze et al., 1996; Kadotani et al., 1996; Takahashi et al., 1996) have suggested that the NR2A and NR2C subunits are present at the mossy fiber synapse at the end of the third postnatal week. Paradoxically, however, previous studies have suggested that the decay time of the NMDAR EPSC is fast regardless of the presence of the NR2C subunit. We now find that at the mature synapse (P40), when the level of NR2C is likely to be high (Monyer et al., 1994) the decay kinetics of the NMDAR EPSC has become slow. As the decay kinetics matched well to the deactivation time of recombinant NR1/NR2C receptors, it seems likely that these receptors predominate at the mature synapse.

Despite the relatively late change in the time course of the NMDAR EPSC, a shift in IC_{50} for Mg^{2+} was apparent by the end of the third postnatal week. This is consistent with the reduced voltage dependence of block that we previously observed in 3-week-old mice (Takahashi et al., 1996). However, the change in Mg^{2+} sensitivity obtained in the present study is less than that described for recombinant NR1/NR2C receptors. In heterologous expression systems the IC_{50} for Mg^{2+} block of NR1/NR2C receptors was approximately six times greater than for NR1/NR2A

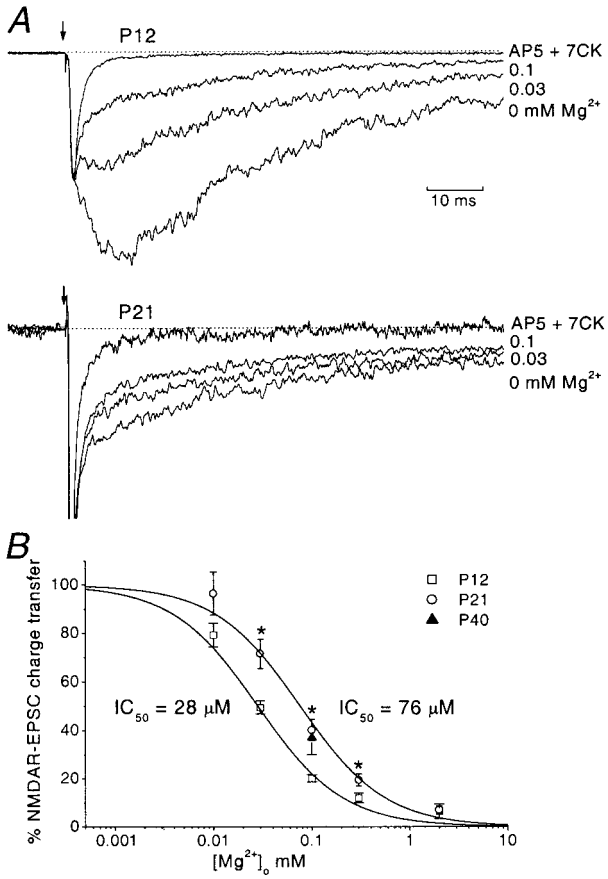

Figure 5. Age-dependent change in sensitivity of the NMDAR EPSC to Mg^{2+}. *A*, Evoked EPSCs at P12 (*top panel*) and P21 (*bottom panel*), recorded in control medium (no added Mg^{2+}) and in the presence of Mg^{2+} (0.03 and 0.1 mM), and in 0 Mg^{2+} plus AP-5 and 7-CK (holding potential, −80 mV). Average traces, obtained at different Mg^{2+} concentrations were normalized to the peak and superimposed to allow a direct comparison of the dose-dependent inhibition of NMDAR EPSCs induced by Mg^{2+}. For clarity only two Mg^{2+} concentrations are depicted at each age (0.03 mM, 0.1 mM). At the end of each experiment 50 μM AP-5 and 50 μM 7-CK were applied to abolish any residual NMDAR-component. The remaining EPSC (the non-NMDAR-component) was subtracted from the traces to allow a direct estimate of charge transfer carried by the NMDAR-component. *B*, Mg^{2+} inhibition curve for NMDAR EPSCs. The mean charge transfer was estimated for each Mg^{2+} concentration: 0.01 mM ($n = 6$ at P12; $n = 4$ at P21), 0.03 mM ($n = 5$ at p12; $n = 10$ at P21), 0.1 mM ($n = 5$ at P12; $n = 10$ at P21; $n = 4$ at P40), 0.3 mM ($n = 11$ at P12, $n = 11$ at P21), and 2 mM ($n = 6$ at P12; $n = 6$ at P21). The NMDAR EPSC, expressed as a percentage of control, was plotted versus Mg^{2+} concentration. Both curves were best fitted by the Hill equation (*black curve*). The IC_{50} values derived from the fit were 28 ± 2 μM at P12 and 76 ± 8 μM at P21 ($p < 0.05$).

or NR1/NR2B assemblies ($V_H = -80$ mV; Kuner and Schoepfer, 1996), compared with our threefold shift. It is of note that when NR2A and NR2C subunits are coexpressed (together with NR1) they exhibit a sensitivity to Mg^{2+} that is appreciably less than for the NR1/NR2A assemblies (Chazot et al., 1994). Indeed, biochemical studies have suggested that coexpression of NR2A and NR2C subunits gives rise to receptors that display a Mg^{2+} sensitivity comparable to that of native cerebellar NMDARs from adult mice (Chazot et al., 1994). It is therefore an attractive possibility that the intermediate IC_{50} that we observe may reflect the presence of triheteromeric NR1/NR2A/NR2C assemblies at the mossy fiber synapse. However, it would be difficult to distinguish between this and the presence of a mixed population of NR2A- and NR2C-containing receptors, especially as it is unclear whether such native receptors would behave in a manner identical to their recombinant counterparts.

The reason why the reduction in Mg^{2+} sensitivity preceded the change in decay kinetics is unclear. One possibility is that a low level of NR2C subunits is sufficient to produce triheteromeric assemblies that may have a reduced Mg^{2+} sensitivity but still exhibit rapid decay kinetics. On the other hand a higher proportion of NR2C may generate sufficient diheteromeric NR1/NR2C assemblies for these to dictate the overall decay time of the NMDAR EPSC. Indeed, there is evidence that the NR2A protein level in granule cells decreases between the third postnatal week and adulthood, whereas the NR2C protein level remains high (Wenzel et al., 1997). This would be consistent with such an interpretation and with the idea that an increased proportion of NR1/NR2C receptors is the primary cause of the slow decay of the mature NMDAR EPSC.

What are the functional consequences of the change in subunit composition of NMDARs at the mossy fiber synapse? NMDARs are critical in triggering activity-dependent synaptic modification (for review, see Gustafsson and Wigstrom, 1988; Malenka and Nicoll, 1999). Developmental changes in receptor expression are therefore likely to have a marked influence on the properties of synaptic plasticity. Many of the cellular functions performed by NMDARs depend on the fact that the open NMDAR channel generates a substantial inward Ca^{2+} current, activating second messengers and intracellular enzymes (MacDermott et al., 1986; Ascher and Nowak, 1988; Jahr and Stevens, 1993; Dingledine et al., 1999). Although NMDAR-dependent long-term potentiation has been identified at the mossy fiber input (D'Angelo et al., 1999), it remains to be seen how the changes in channel kinetics and Mg^{2+} sensitivity influence the coincidence detection behavior of the synaptic NMDARs at the mature synapse. In the visual cortex, the experience-dependent acceleration of the NMDAR EPSC, which occurs during development, results from a switch between NR2B- and NR2A-containing NMDARs (Quinlan et al., 1999) and correlates with a modification in the long-term depression/long-term potentiation threshold, making long-term depression more likely (Kirkwood et al., 1996). It will be of interest to see whether a developmental modification of long-term changes also occurs at granule cell synapses.

Recent studies have indicated that both native NR1/NR2C- and NR1/NR2D receptors (like their recombinant counterparts) give rise to channels with unique properties. These include a low conductance and a low sensitivity to block by Mg^{2+} ions, when compared with "conventional" NMDARs (Momiyama et al., 1996; Cull-Candy et al., 1998). If present at synapses, these receptors could therefore operate as "low-threshold" NMDAR channels, because their weak Mg^{2+} block would be more readily alleviated by membrane depolarization. Despite the widespread occurrence of functional NR2D-containing NMDARs in the extrasynaptic membrane of neurons, there is little direct evidence that NR1/NR2D receptors are targeted to synaptic sites (Bardoni et al., 1998; Misra et al., 2000a). Indeed, there are no reports of synaptic responses with decay times comparable to the deactivation rate for native NR1/NR2D receptors (Misra et al., 2000b). It is therefore of particular interest that the other type of NR2 subunit giving rise to low-conductance channels appears to determine key properties of the NMDAR EPSCs in mature granule cells.

REFERENCES

Akazawa C, Shigemoto R, Bessho Y, Nakanishi S, Mizuno N (1994) Differential expression of five *N*-methyl-D-aspartate receptor subunit mRNAs in the cerebellum of developing and adult rats. J Comp Neurol 347:150–160.

Ascher P, Nowak L (1988) The role of divalent cations in the *N*-methyl-D-aspartate responses of mouse central neurones in culture. J Physiol (Lond) 399:247–266.

Bardoni R, Magherini PC, MacDermott AB (1998) NMDA EPSCs at glutamatergic synapses in the spinal cord dorsal horn of the postnatal rat. J Neurosci 18:6558–6567.

Carmignoto G, Vicini S (1992) Activity-dependent decrease in NMDA receptor responses during development of the visual cortex. Science 258:1007–1011.

Chazot PL, Coleman SK, Cik M, Stephenson FA (1994) Molecular characterisation of *N*-methyl-D-aspartate receptors expressed in mammalian cells yields evidence for the coexistence of three subunit types within a discrete receptor molecule. J Biol Chem 269:24403–24409.

Clark BA, Farrant M, Cull-Candy SG (1997) A direct comparison of the

single-channel properties of synaptic and extrasynaptic NMDA receptors. J Neurosci 17:107–116.
Cull-Candy SG, Brickley SG, Misra C, Feldemeyer D, Momiyama A, Farrant M (1998) NMDA receptor diversity in the cerebellum: identification of subunits contributing to functional receptors. Neuropharmacology 37:1369–1380.
D'Angelo E, Rossi P, Taglietti V (1993) Different proportions of *N*-methyl-D-aspartate and non-*N*-methyl-D-aspartate receptor currents at the mossy fiber-granule cell synapse of developing rat cerebellum. Neuroscience 53:121–130.
D'Angelo E, Rossi P, Armano S, Taglietti V (1999) Evidence for NMDA and mGlu receptor-dependent long-term potentiation of mossy fiber-granule cell transmission in rat cerebellum. J Neurophysiol 81:277–287.
Dingledine R, Borges K, Bowie D, Traynelis SF (1999) The glutamate receptor ion channels. Pharmacol Rev 51:7–61.
Ebralidze AK, Rossi DJ, Tonegawa S, Slater NT (1996) Modification of NMDA receptor channels and synaptic transmission by targeted disruption of the NR2C gene. J Neurosci 16:5014–5025.
Farrant M, Feldmeyer D, TakahashiT, Cull-Candy SG (1994) NMDA-receptor channel diversity in the developing cerebellum. Nature 368:335–339.
Feldmeyer D, Cull-Candy S (1996) Functional consequences of changes in NMDA receptor subunit expression during development. J Neurocytol 25:857–867.
Gallagher MJ, Huang H, Pritchett DB, Lynch DR (1996) Interactions between ifenprodil and the NR2B subunit of the *N*-methyl-D-aspartate receptor. J Biol Chem 271:9603–9611.
Gustafsson B, Wigstrom H (1988) Physiological mechanisms underlying long-term potentiation. Trends Neurosci 11:156–162.
Hamori J, Somogyi J (1983) Differentiation of cerebellar mossy fiber synapses in the rat: a quantitative electron microscope study. J Comp Neurol 220:365–377.
Hestrin S (1992) Developmental regulation of NMDA mediated synaptic currents at a central synapse. Nature 357:686–689.
Jahr CE, Stevens CF (1993) Calcium permeability of the *N*-methyl-D-aspartate receptor channel in hippocampal neurons in culture. Proc Natl Acad Sci USA 90:11573–11577.
Kadotani H, Hirano T, Masugi M, Nakamura K, Nakao K, Katsuki M, Nakanishi S (1996) Motor discoordination results from combined gene disruption of the NMDA receptor NR2A and NR2C subunits, but not from single disruption of the NR2A or NR2C subunit. J Neurosci 16:7859–7867.
Kirkwood A, Rioult MG, Bear MF (1996) Experience-dependent modification of synaptic plasticity in visual cortex. Nature 381:526–528.
Kuner T, Schoepfer R (1996) Multiple structural elements determine subunit specificity of Mg^{2+} block in NMDA receptor channels. J Neurosci 16:3549–3558.
Legendre P, Westbrook GL (1991) Ifenprodil blocks *N*-methyl-D-aspartate receptors by a two-component mechanism. Mol Pharmacol 40:289–298.
MacDermott AB, Mayer ML, Westbrook GL, Smith SJ, Barker JL (1986) NMDA-receptor activation increases cytoplasmic calcium concentration in cultured spinal cord neurones. Nature 321:519–522.
Malenka RC, Nicoll RA (1999) Long-term potentiation—a decade of progress? Science 285:18701–1874.
Mayer ML, Westbrook GL, Guthrie PB (1984) Voltage-dependent block by Mg^{2+} of NMDA responses in spinal cord neurones. Nature 309:261–263.
Misra C, Brickley S, Farrant M, Cull-Candy SG (2000a) Identification of subunits contributing to synaptic and extrasynaptic NMDA receptors in Golgi cells of the rat cerebellum. J Physiol (Lond) 524:147–162.
Misra C, Brickley S, Farrant M, Cull-Candy SG (2000b) Slow deactivation kinetics of NMDA receptors containing NR1 and NR2D subunits in rat cerebellar Purkinje cells. J Physiol (Lond) 525:299–305.
Momiyama A, Feldmeyer D, Cull-Candy SG (1996) Identification of a native low-conductance NMDA channel with reduced sensitivity to Mg^{2+} in rat central neurones. J Physiol (Lond) 494:479–492.
Monyer H, Burnashev N, Laurie DJ, Sakmann B, Seeburg PH (1994) Developmental and regional expression in the rat brain and functional properties of four NMDA receptors. Neuron 12:529–540.
Nowak L, Bregestovski P, Ascher P, Herbet A, Prochiantz A (1984) Magnesium gates glutamate-activated channels in mouse central neurones. Nature 307:462–465.
Paoletti P, Ascher P, Neyton J (1997) High-affinity zinc inhibition of NMDA NR1-NR2A receptors. J Neurosci 17:5711–5725.
Priestley T, Laughton P, Myers J, Le Bourdelles B, Kerby J, Whiting PJ (1995) Pharmacological properties of recombinant human *N*-methyl-D-aspartate receptors comprising NR1a/NR2A and NR1a/NR2B subunit assemblies expressed in permanently transfected mouse fibroblast cells. Mol Pharmacol 48:841–848.
Quinlan EM, Philpot BD, Huganir RL, Bear MF (1999) Rapid, expression-dependent expression of synaptic NMDA receptors in visual cortex in vivo. Nat Neurosci 2:352–357.
Roberts EB, Ramoa AS (1999) Enhanced NR2A subunit expression and decreased NMDA receptors decay time at the onset of ocular dominance plasticity in the ferret. J Neurophysiol 81:2587–2591.
Rumbaugh G, Vicini S (1999) Distinct synaptic and extrasynaptic NMDA receptors in developing cerebellar granule neurons. J Neurosci 19:10603–10610.
Silver RA, Traynelis SF, Cull-Candy SG (1992) Rapid-time-course miniature and evoked excitatory currents at cerebellar synapses in situ. Nature 355:163–166.
Silver RA, Cull-Candy SG, Takahashi T (1996) Non-NMDA glutamate receptor occupancy and open probability at a rat cerebellar synapse with single and multiple release sites. J Physiol (Lond) 494:231–250.
Stocca G,Vicini S (1998) Increased contribution of NR2A subunit to synaptic NMDA receptors in developing rat cortical neurons. J Physiol (Lond) 507:13–24.
Takahashi T, Feldmeyer D, Suzuki N, Onodera K, Cull-Candy SG, Sakimura K, Mishina M (1996) Functional correlation of NMDA receptor epsilon subunit expression with the properties of single-channel and synaptic currents in the developing cerebellum. J Neurosci 16:4376–4382.
Tovar KR, Westbrook GL (1999) The incorporation of NMDA receptors with a distinct subunit composition at nascent hippocampal synapses in vitro. J Neurosci 19:4180–4188.
Vicini S, Wang JF, Li JH, Zhu WJ, Wang YH, Luo JH, Wolfe BB, Grayson DR (1998) Functional and pharmacological differences between recombinant NMDA receptors. J Neurophysiol 79:555–566.
Watanabe M, Mishina M, Inoue Y (1994) Distinct spatiotemporal distributions of the *N*-methyl-D-aspartate receptor channel subunit mRNAs in the mouse cervical cord. J Comp Neurol 345:314–319.
Wenzel A, Fritschy JM, Mohler H, Benke D (1997) NMDA receptor heterogeneity during postnatal development of the rat brain: differential expression of the NR2A, NR2B, and NR2C subunit proteins. J Neurochem 68:469–478.
Williams K (1993) Ifenprodil discriminates subtypes of the *N*-methyl-D-aspartate receptor: selectivity and mechanisms at recombinant heteromeric receptors. Mol Pharmacol 44:851–859.
Williams K (1995) Pharmacological properties of recombinant *N*-methyl-D-aspartate (NMDA) receptors containing the epsilon 4 (NR2D) subunit. Neurosci Lett 184:181–184.
Wyllie DJA, Béhé P, Colquhoun D (1998) Single-channel activations and concentration jumps: comparison of recombinant NR1a/NR2A and NR1a/NR2D NMDA receptors. J Physiol (Lond) 510:1–18.